ACS APPLIED MATERIALS & INTERFACES

Research Article

www.acsami.org

Temperature-Switchable Agglomeration of Magnetic Particles Designed for Continuous Separation Processes in Biotechnology

Anja S. Paulus,* Raphael Heinzler, Huey Wen Ooi, and Matthias Franzreb

Institute of Functional Interfaces (IFG), Karlsruhe Institute of Technology (KIT), Hermann-von-Helmholtz-Platz 1, 76344 Eggenstein-Leopoldshafen, Germany

Supporting Information

ABSTRACT: The purpose of this work was the synthesis and characterization of thermally switchable magnetic particles for use in biotechnological applications such as protein purification and enzymatic conversions. Reversible addition−fragmentation chain-transfer polymerization was employed to synthesize poly(*N*-isopropylacrylamide) brushes via a "graft-from" approach on the surface of magnetic microparticles. The resulting particles were characterized by infrared spectroscopy and thermogravimetric analysis and their temperature-dependent agglomeration behavior was assessed. The influence of several factors on particle agglomeration (pH, temperature, salt type, and particle concentration) was evaluated. The results showed that a low pH value (pH 3−4), a kosmotropic salt (ammonium sulfate), and a high particle concentration (4 g/L) resulted in improved agglomeration at elevated temperature (40 °C). Recycling of particles and reversibility of the temperature-switchable agglomeration were successfully demonstrated for ten heating−cooling cycles. Additionally, enhanced magnetic separation was observed for the modified particles. Ionic monomers were integrated into the polymer chain to create end-group functionalized particles as well as two- and three-block copolymer particles for protein binding. The adsorption of lactoferrin, bovine serum albumin, and lysozyme to these ion exchange particles was evaluated and showed a binding capacity of up to 135 mg/g. The dual-responsive particles combined magnetic and thermoresponsive properties for switchable agglomeration, easy separability, and efficient protein adsorption.

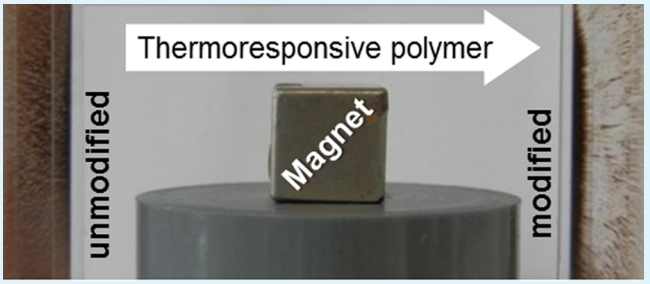

KEYWORDS: *stimuli-responsive material, thermoresponsive polymer, magnetic microparticles, poly(N-isopropylacrylamide), block copolymer, bioseparation process*

1. INTRODUCTION

In the past decade, much work has been done to design and develop magnetic particles that not only possess magnetic properties, but also have the ability to respond rapidly to small changes in their environment.[1,2] Stimuli-responsive magnetic particles have shown potential in numerous applications due to their ability to react to external parameters, such as temperature, pH, ionic strength and many more. Thermosensitive magnetic particles, in particular, have been applied as adsorbents in separation processes,[3,4] drug delivery,[5,6] microfluidic devices,[7] emulsion stabilization,[8] and enzyme immobilization.[9] In comparison to commonly used techniques such as filtration, precipitation, and chromatography, magnetic-based separation is a simple yet economical technique that has shown promising potential in the separation of biomolecules.

Poly(*N*-isopropylacrylamide) (PNIPAM) is the most widely used thermoresponsive polymer.[10] It is suitable for biotechnological applications because of its lower critical solution temperature (LCST) of approximately 32 °C.[11] The chemical modification of particles by polymer chains can be accomplished by either the "graft-to" or the "graft-from" approach.[12] While the "graft-to" synthesis allows a-priori characterization of the polymer, higher grafting densities can be achieved with the "graft-from" approach.[13] The reversible addition−fragmentation chain-transfer (RAFT) polymerization technique is a form of reversible-deactivation radical polymerization, which allows syntheses of polymers with narrow molar mass dispersity and predetermined molecular weight.[14] In addition, RAFT polymerization also provides the flexibility to prepare complex molecular architectures (stars, blocks, and networks) through end-group modification and chain extension reactions. For example, a combination of "graft-from" and RAFT polymerization was previously employed by Ma et al.[15] who modified silica nanoparticles with an optimized ratio of copolymerized polyethylene glycol and positively charged quaternary amines for drug delivery. Lai et al.[7] synthesized thermoresponsive magnetic nanoparticles (via RAFT polymerization, self-assembly, and cross-linking) and demonstrated reversible aggregation in a microfluidic device at a temperature above the LCST.

Ion-exchange polymers, which provide affinity toward specific biomolecules, can be incorporated onto magnetic

Received: March 26, 2015
Accepted: June 12, 2015
Published: June 12, 2015

DOI: 10.1021/acsami.5b02642
ACS Appl. Mater. Interfaces 2015, 7, 14279−14287

particles for protein purification and separation. These ion-exchange moieties have the ability to protonate/deprotonate depending on changes in pH, subsequently allowing the adsorption/desorption of proteins through electrostatic interactions. Negatively charged carbonyl groups of acrylic acid (AA) comonomers were utilized by Borlido and co-workers to prepare cross-linked P(NIPAM-*co*-AA) with magnetic nanoparticles core for purification of monoclonal antibodies.[4] Rahman et al.[16] reported the use of magnetic particles coated with cross-linked P(NIPAM-*co*-aminoethyl methacrylate) shell for DNA separation through electrostatic interactions. DNA adsorption was observed to be dependent on the net surface charge and density of the particles. Furthermore, magnetic nanoparticles grafted with P(NIPAM-*co*-(1-(N,N-bis-carboxymethyl)amino-3-allylglycerol)) have shown success in solid phase extraction and determination of trace fluvoxamine in biological human fluids and pharmaceutical samples.[17]

In this work, we present the synthesis and characterization of dual-responsive magnetic particles via the "graft-from" RAFT polymerization approach for continuous bioseparation processes. Our particles consist of a magnetic core and a thermoresponsive PNIPAM polymer shell, which was further chain extended with a second block of ion-exchange copolymer, poly(2-sulfopropyl acrylate) (PSPA) and poly(2-carboxyethyl acrylate) (PCEA), to create protein binding sites. Through this design, proteins can be captured by the well-dispersed M-P(NIPAM-SPA) and M-P(NIPAM-CEA) magnetic particles at ambient conditions and enhanced separation of the proteins can be carried out in a magnetic field at a temperature above its phase transition temperature.

2. EXPERIMENTAL PROCEDURE

2.1. Materials. Commercially available magnetic microparticles (approximately 1−3 μm) were used in all experiments (M-PVA 012; PerkinElmer chemagen Technologie GmbH, Baesweiler, Germany). They consist of nanometer sized magnetite crystals encapsulated in a hydrophilic matrix of cross-linked poly(vinyl alcohol). These particles show a relatively high magnetization and superparamagnetic behavior (see Figure S1 in the Supporting Information for magnetic characterization), which are favorable properties for magnetic particles to be used repeatedly in a separation process. Additional data on particle characterization can be found in the Supporting Information.

Methanol (≥99.9%, Carl Roth, Germany), acetone (≥99%, Merck, Germany), *n*-hexane (≥97%, Sigma-Aldrich, USA), 1,4-dioxane (99.8%, VWR, USA), tetrahydrofuran (THF, ≥ 99.9%, Merck, Germany), diethyl ether (≥99%, VWR), and N,N-dimethylformamide (DMF, 99.5%, Merck) were used as received. *N*-isopropylacrylamide (NIPAM, 97%, Sigma-Aldrich) was recrystallized in *n*-hexane before use. 2,2′-Azobis(2-methylpropionitrile) (AIBN, ≥ 98%, Sigma-Aldrich) was recrystallized in methanol and used as an initiator for the RAFT reaction. The chain transfer agent 2-(Dodecylthiocarbonothioylthio)-2-methylpropionic acid (DMP) was synthesized according to Lai et al.[18] 3-Sulfopropyl acrylate potassium salt (SPA) and 2-carboxyethyl acrylate (CEA) were used as copolymer units with cation exchange functionality and were purchased from Sigma-Aldrich. The inhibitor present in CEA was removed by filtration through a basic aluminum oxide column. 4-(Dimethylamino)pyridine (DMAP), 1-ethyl-3-(3-dimethylaminopropyl)carbodiimide hydrochloride (EDC), and triethylamine (TEA) were purchased from Merck. Tris(2-carboxyethyl)phosphine hydrochloride (TCEP, 98%, Alfa Aesar, USA) was used as a reducing agent during end-group modification. Ammonium sulfate (>99%), disodium hydrogen phosphate (>99%), sodium chloride (>99%), and sodium dihydrogen phosphate (>98%) were purchased from Merck and potassium iodide (99%) was purchased from Applichem (Germany).

The proteins lysozyme (hen egg white, ≥ 90%, Sigma-Aldrich), lactoferrin (bovine whey, 97%, Milei GmbH, Germany), and albumin (bovine serum, ≥ 98%, Merck) were used for adsorption studies. All buffers were prepared with deionized water.

2.2. Synthesis of PNIPAM-Functionalized Magnetic Particles [M-PNIPAM]. First, DMP-functionalized M-PVA particles were prepared by adding 30 mg of M-PVA 012 particles, DMP (52.5 mg, 144 μmol), EDC (55.2 mg, 288 μmol), DMAP (1.8 mg, 14 μmol), and DMF (0.5 mL) into a 1.5 mL microtube. The reaction solution was incubated at 25 °C in a shaker (1400 rpm) for 17 h. The DMP-functionalized particles were magnetically separated from the reaction solution, followed by washing with DMF (1 mL × 3), acetone (1 mL × 2), deionized water at 50 °C (1 mL × 2), 1 M NaCl in 0.1 M phosphate buffer pH 7 (1 mL), deionized water (1 mL × 2), acetone (1 mL), and 1,4-dioxane (1 mL). After every washing step, magnetic separation was used to collect the particles.

M-PNIPAM was synthesized with two different chain lengths of PNIPAM, 17 kDa and 30 kDa. The resultant DMP-functionalized particles were transferred to a 10 mL glass tube while a solution of NIPAM (17 kDa, 1 g/8.4 mmol; 30 kDa, 3.6 g/31.8 mmol) and AIBN (17 kDa, 1 mg/5.98 μmol; 30 kDa, 2 mg/12 μmol) in 1,4-dioxane (17 kDa, 2.25 mL; 30 kDa, 8.12 mL) was prepared in a separate glass vial. Additional DMP (10.92 mg, 29.94 μmol) was added to synthesize free PNIPAM chains which lowers the polydispersity and prevents interparticle coupling.[19] The monomer solution was then added to the glass tube with the particles and sealed with a rubber septum. The reaction solution was deoxygenated with nitrogen for 30 min. Polymerization was then carried out for 17 h in a 60 °C water bath equipped with a shaker (200 rpm). The reaction was stopped by cooling the reaction vessel in an ice bath. A sample of the reaction supernatant was taken for further analysis (NMR, GPC). The M-PNIPAM particles were magnetically separated from the reaction solution and washed with 1,4-dioxane (1 mL × 3), deionized water at 50 °C (1 mL × 2), 1 M NaCl in 0.1 M phosphate buffer pH 7 (1 mL), deionized water (1 mL × 2), and acetone (1 mL). Again, magnetic separation was used after every washing step to separate the particles from the reaction medium. Particles were left to dry at ambient conditions.

2.3. End-Group Modification of M-PNIPAM [M-PNIPAM-CEA and M-PNIPAM-SPA]. First, the M-PNIPAM 17 kDa particles (30 mg) were washed with deionized water (1 mL × 2), DMF (1 mL), and THF (1 mL). To these particles, hexylamine (63.9 μL, 480 μmol) and TCEP (6.9 mg, 24 μmol) were added. The particles were incubated for 30 min at 25 °C under a nitrogen atmosphere.

To prepare M-PNIPAM end-groups modified with SPA, this was followed by addition of TEA (3.33 μL, 24 μmol) and SPA (55.8 mg, 240 μmol), which was first dissolved in deionized water (0.2 mL). THF (1 mL) was added as solvent. The particles were then incubated for 18 h at 25 °C under nitrogen atmosphere. The particles were magnetically separated from the reaction solution and washed with deionized water (1 mL × 2), reaction solvent (1 mL × 2), and deionized water (1 mL × 2). CEA end-group functionalized particles were also prepared in the similar method, with the addition of 2-carboxyethyl acrylate (34.6 mg, 240 μmol) instead of SPA and DMF was used as solvent.

2.4. Syntheses of Block Copolymers. *2.4.1. Two-Block Copolymers [M-P(NIPAM-SPA) and M-P(NIPAM-CEA)].* In a glass tube with M-PNIPAM (30 mg), the acrylate (115.2 mg/496.0 μmol of SPA or 71.5 mg/495.8 μmol of CEA), which was first dissolved in deionized water (0.2 mL), and AIBN (0.8 mg, 4.8 μmol) were added to the particles and dissolved in DMF (1.5 mL). The tube was sealed with a rubber septum and was purged with nitrogen for 30 min before incubated for 18 h at 60 °C. The polymerization was stopped by cooling the reaction vessel in an ice bath. The particles were washed with DMF (1 mL × 2), 1 M NaCl in 0.1 M phosphate buffer pH 7 (1 mL), deionized water at 50 °C (1 mL × 2), and acetone (1 mL × 2).

2.4.2. Three-Block Copolymers [M-P(NIPAM-SPA-NIPAM)]. In a glass tube containing M-P(NIPAM-SPA) particles (30 mg), NIPAM (510 mg, 4.5 mmol), and AIBN (0.8 mg, 6 μmol) were added and dissolved in 1,4-dioxane (2 mL). The tube was sealed with a rubber

DOI: 10.1021/acsami.5b02642
ACS Appl. Mater. Interfaces 2015, 7, 14279−14287

septum and purged with nitrogen for 30 min before incubated for 18 h at 60 °C. The polymerization was stopped by cooling the reaction vessel in an ice bath. The M-P(NIPAM-SPA-NIPAM) particles were washed with DMF (1 mL × 2), 1 M NaCl in 0.1 M phosphate buffer pH 7 (1 mL), deionized water at 50 °C (1 mL × 2), and acetone (1 mL).

2.5. ATR-FTIR Spectroscopy. Attenuated total reflection (ATR) Fourier-transform infrared (FTIR) spectroscopy was applied in this work to analyze the magnetic particles for new molecules and bonds. Approximately 5 mg of particles were washed with 0.1 M MES buffer pH 5.3 (1 mL × 2) and deionized water (1 mL × 2), before they were magnetically separated and dried overnight at 60 °C. A Fourier-transform infrared spectrometer with an attenuated total reflection unit (Tensor 27 and Platinum ATR accessory, Bruker Optics, Germany) was used for measurement of particle samples. The spectra were recorded from 4000 to 400 cm^{-1} at a resolution of 4 cm^{-1} using 32 scans per measurement and were evaluated with the software OPUS (Version 7.2, Bruker Optics).

2.6. Thermogravimetric Analysis (TGA). The polymer content of unfunctionalized and PNIPAM functionalized magnetic particles was determined by thermogravimetric analysis (TGA).[20] A defined mass (approximately 5 mg) of predried particles was measured in a thermal analyzer STA 449 C (Netzsch, Germany) under N_2 flow (20 mL/min) with a heating rate of 10 K/min up to a temperature of 1000 °C. The sample mass was recorded as a function of the temperature and mass spectroscopy of the volatile decomposition products (QMS 403 C, Netzsch) was run in parallel. Using a simple calculation, the polymer content of the particles can be determined under the assumption that the polymer is completely decomposed and evaporated. First, the magnetite mass fraction of particles is determined from the initial (at 50 °C) and residual mass (at 700 °C) of the particle sample, $m_{0,\text{ particle}}$ and $m_{r,\text{ particle}}$, respectively

$$\xi_{\text{magnetite,particle}} = \frac{m_{\text{r,particle}}}{m_{\text{0,particle}}} \tag{1}$$

The PVA mass fraction of the M-PVA particles directly follows from the mass balance of the M-PVA particles

$$\xi_{\text{PVA,M-PVA}} = 100\% - \xi_{\text{magnetite,M-PVA}} \tag{2}$$

As the PVA to magnetite ratio of all particles is constant, it can be used to calculate the fraction of PVA in M-PNIPAM and M-P(NIPAM-SPA) particles. The PNIPAM mass fraction $\xi_{\text{PNIPAM, M-PNIPAM}}$ is then calculated by a mass balance of the M-PNIPAM particles

$$\xi_{\text{PNIPAM,M-NIPAM}} = 100\% - \xi_{\text{PVA,M-PNIPAM}} - \xi_{\text{magnetite,M-PNIPAM}} \tag{3}$$

As the M-P(NIPAM-SPA) particles were synthesized from the M-PNIPAM particles, the ratio of PNIPAM to magnetite is constant as well. This allows calculation of the PNIPAM mass fraction of M-P(NIPAM-SPA) particles. The PSPA mass fraction ξ_{PSPA} is again calculated by a simple mass balance of the particle.

2.7. Agglomeration Behavior. UV/vis transmission measurements were carried out with a UVmini-1240 spectrophotometer (Shimadzu, Japan) at a defined temperature. First, a blank sample containing only buffer was measured to set the transmission to 100%. Then, 2 mL particle suspension was filled into a cuvette and placed inside the spectrophotometer's temperature-regulated measurement chamber. After 10 min, the sample was resuspended and the transmission at 500 nm was recorded every 15 s over an interval of 3 min. These observations are intended to show the formation of agglomerates and the sediment of particles and agglomerates due to gravity. Because the light path through the cuvette is perpendicular to the sedimentation of the particle sample, the transmission will increase over time. The transmission values were normalized to the initial transmission value at time 0 s.

2.8. Recycling Experiments. Repeated agglomeration and recycling of particles was investigated using the following procedure: a sample of 2 mL of particle suspension was filled into a cuvette, cooled to 20 °C for 10 min. After resuspension and 3 min of sedimentation, the transmission at 500 nm was recorded. The sample was then heated to 40 °C for 10 min, resuspended and the transmission was again recorded after 3 min of settling. Next, the cuvette with the sample was weighed, the particles were magnetically separated, and the supernatant was removed. The sample was filled up with fresh buffer to the initial weight. These steps were repeated nine times and the transmission values were plotted versus the number of cycles.

2.9. Magnetic Separation. Magnetic separation of particles was conducted using a small permanent magnet. The particle sample in buffer was filled into rectangular sample cells (LUM GmbH, Germany) with a path length of 2 mm. First, the temperature of the suspension was equilibrated for 10 min, and then the sample was resuspended and placed next to the magnet at a defined distance (3 cm). Magnetic separation was observed visually and documented with a camera.

2.10. Protein Adsorption Studies. The protein adsorption capacity of particles was determined in a 1 mL scale with lactoferrin, lysozyme, and bovine serum albumin (BSA) as model enzymes. The protein loading of particles Q (mg protein/g particle) was determined for a defined temperature and calculated following eq 4

$$Q = \frac{(c_0 - c^*)V_{\text{total}}}{m_{\text{p}}} \tag{4}$$

with the particle mass m_p, the protein concentration in the initial solution c_0, and in the supernatant c^* after 30 min of equilibration, and the total volume of the sample V_{total}. The protein concentration was determined by UV/vis absorption measurements at 280 nm.

Different temperatures (20 and 40 °C) were used during adsorption to examine the effects of the PNIPAM chain conformation (linear, collapsed) on adsorption behavior. The Langmuir isotherm was fitted to the data points

$$Q = Q_{\text{max}}\frac{c^*}{k_{\text{L}} + c^*} \tag{5}$$

with the equilibrium loading and maximum loading of the adsorber Q and Q_{max}, the equilibrium concentration c^* and the Langmuir coefficient k_L. For particles that did not follow the simple Langmuir equation, a Bi-Langmuir fit of the following form was used

$$Q = a\frac{c^*}{b + c^*} + c\frac{c^*}{d + c^*} \tag{6}$$

where a, b, c, and d are the fitting parameters of the two individual Langmuir terms. In eq 6, the first term serves to describe low, unspecific binding, while the second term serves to explain high specific binding to the ligands of the adsorbents. The software SigmaPlot, version 11.0, (Systat Software Inc., USA) was used for data fitting. The desorption yield was defined as the fraction of desorbed protein using 1 M NaCl as an eluting agent.

For particles with low protein binding capacity, fluorescence microscopy was employed using an Axio Observer Z1 at 63× magnification with filter set 81 HE (Zeiss, Germany). Adsorption of green fluorescent protein (GFP) to unmodified, PNIPAM modified and end-group functionalized particles was investigated. The particles (approximately 2 mg) were incubated in 500 μL of GFP solution (approximately 1.5 g/L in 10 mM acetate buffer pH 4) for 30 min at 18 °C. Next, the supernatant was removed and the particles were washed with pure buffer and subsequently diluted in ethanol. A small volume (3 μL) of dilute particle suspension was transferred to a microscope slide were the solvent was allowed to evaporate. Then, 10 μL of stabilizing fluid (Fluoroshield Mounting, Abcam, UK) were added on the sample and a cover glass was put on top. Still images were recorded both in bright field and using the green filter (470 nm). The software ZEN lite (Zeiss) was used for image analysis.

DOI: 10.1021/acsami.5b02642
ACS Appl. Mater. Interfaces 2015, 7, 14279−14287

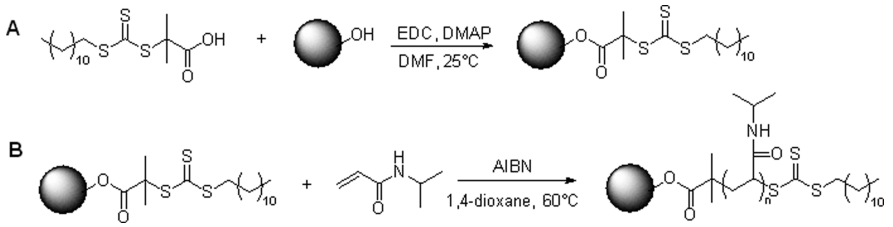

Figure 1. Reaction scheme of (A) the attachment of DMP onto the particles, followed by (B) the "graft-from" RAFT polymerization of NIPAM.

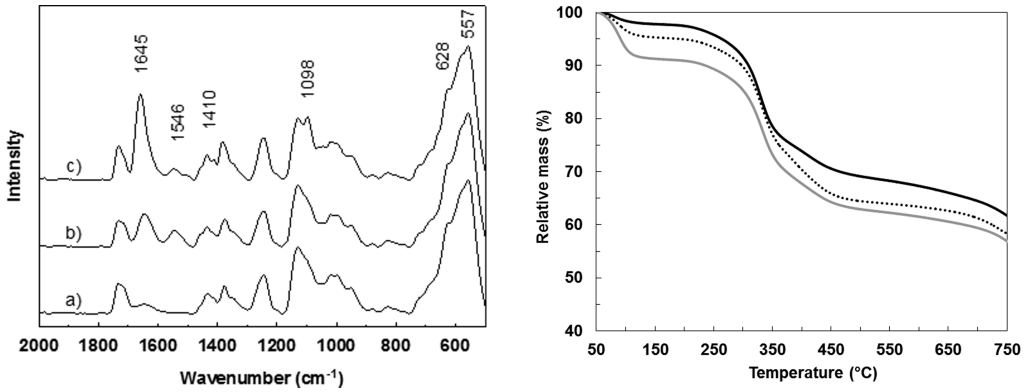

Figure 2. ATR-FTIR spectra (left) of (a) unmodified M-PVA, (b)M-PNIPAM 17 kDa, and (c) P(NIPAM-SPA) particles in the range 500−2000 cm^{-1}. Relevant peaks are indicated by their wavenumber. Thermogravimetric analysis (right) of unmodified M-PVA magnetic particles (solid black line) and M-PNIPAM 17 kDa (dotted black line), and M-P(NIPAM-SPA) (solid gray line) thermoresponsive particles. The relative mass is based on the initial mass of the sample at 50 °C and is plotted versus the temperature.

3. RESULTS AND DISCUSSION

In the following sections, the chemical surface structures of thermoresponsive magnetic microparticles of different complexity are characterized in detail, followed by the discussion of the effects of surface chemistry onto temperature-induced agglomeration behavior and protein binding capabilities. This will be done step by step, starting from the properties of unmodified, commercial magnetic microparticles having a plain poly(vinyl alcohol) matrix (M-PVA) with embedded magnetite nanocrystals, followed by the same particles with *N*-isopropylacrylamide polymer chains grafted to their surface (M-PNIPAM), toward two-block polymer particles having a chain extension of the PNIPAM with a second block of ion-exchange copolymer, either poly(3-sulfopropyl acrylate M-P(NIPAM-SPA) or poly-(2-carboxyethyl acrylate M-P(NIPAM-CEA), and finally, three-block polymers having a further PNIPAM block coupled onto M-P(NIPAM-SPA) particles, resulting in a M-P(NIPAM-SPA-NIPAM) structure.

3.1. M-PNIPAM Particles. The reaction scheme for the RAFT "graft-from" synthesis of PNIPAM on magnetic particles is shown in Figure 1. First, the RAFT chain transfer agent (DMP) was bound to the particle surface via Steglich esterification at 25 °C, followed by RAFT polymerization of NIPAM. ATR-IR spectroscopy confirmed the successful introduction of PNIPAM chains. Figure 2 (left) shows the spectra of unmodified and modified particles in the range 500−2000 cm^{-1}. No change is observed for wavenumbers 628 and 557 cm^{-1} where magnetite shows characteristic bands, so that it can be concluded that the magnetic particle itself is preserved. New bands are visible at 1645 cm^{-1} and at 1546 cm^{-1} which are characteristic for amide I and amide II bands, respectively.[21] Since PNIPAM chains contain amide bonds, it can be concluded that the polymer is present. For P(NIPAM-SPA) particles, new bands appear at 1410 and 1098 cm^{-1} that can be attributed to stretching of SO_3^- from the newly introduced SPA.[22]

Thermogravimetric analysis (TGA) allows a comparison of temperature profiles and the residual mass of different particles. The relative mass as a function of temperature for M-PVA, M-PNIPAM 17 kDa, and M-P(NIPAM-SPA) particles is shown in Figure 2 (right). It can be concluded that the polymer (PVA, PNIPAM, and PSPA) is mainly degraded between 300 and 400 °C,[23,24] whereas the remaining magnetite undergoes further transformation up to a temperature of 1000 °C.[25] Mass spectroscopy of CO_2, H_2O, and SO_2 was run in parallel with TGA (see the Supporting Information, Figure S6). These data indicate that respective polymers were fully decomposed below 700 °C. The PNIPAM mass fraction ξ of the M-PNIPAM particles was calculated to approximately 5% using eq 3. The PNIPAM and PSPA mass fractions of M-P(NIPAM-SPA) particles were calculated to approximately 5 and 3%, respectively.

A sample of the PNIPAM chains in the sorption supernatant was characterized further via NMR and GPC (see the Supporting Information). The molecular weight of the polymer in the supernatant can be used to approximate the molecular weight of the attached polymer chains.[19] The actual molecular weight of the PNIPAM chains of the M-PNIPAM 17 kDa and 30 kDa synthesis procedures was determined to approximately 45 kDa and 63 kDa, respectively. The polydispersity of the samples was low (PDI: approximately 1.2). The grafting density was calculated to approximately 0.026 polymer chains per nm^2 of particle surface. Therefore, one polymer chain occupies an area of approximately 38 nm^2, resulting in an average chain distance of approximately 6 nm. From this number, it can be assumed that the distance between polymer chains is bigger than their gyration radius, and the chains form mushroomlike

DOI: 10.1021/acsami.5b02642
ACS Appl. Mater. Interfaces 2015, 7, 14279−14287

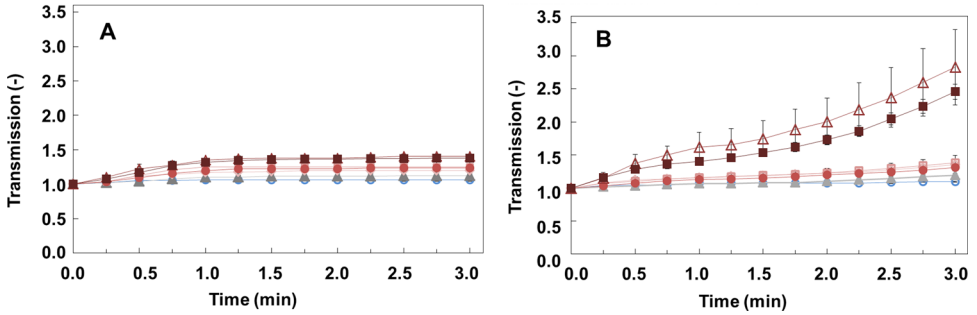

Figure 3. Normalized transmission of (A) M-PVA and (B) M-PNIPAM 17 kDa particle suspensions recorded over time at 500 nm. Testing was done at pH 7 in 0.1 M phosphate buffer at a particle concentration of 4 g/L and the suspension temperature was varied (empty circles, 25 °C; filled triangles, 30 °C; empty squares, 34 °C; filled circles, 36 °C; empty triangles, 38 °C; filled squares, 40 °C).

structures that do not exclude larger molecules from approaching lower parts of the chain.

Both TGA and ATR-IR analysis show that the polymer is present in M-PNIPAM particles. Therefore, the thermoresponsive property of these modified particles was investigated. The dependence of particle agglomeration behavior on various factors is discussed in the following.

3.1.1. Effect of Temperature on Particle Agglomeration. The effect of temperature on particle agglomeration was studied with suspensions of varied temperature (30–40 °C, reference at 25 °C). Figure 3 shows the transmission of M-PVA (A) and M-PNIPAM 17 kDa (B) suspensions at 500 nm over time. At low temperatures, the transmission is nearly constant for both types of particles. The transmission of M-PNIPAM suspensions reaches higher values with increasing temperatures which indicates that agglomeration of particles increases likewise. This is a result of the collapse of PNIPAM chains that takes place around the LCST. In this case, a distinct change in behavior is seen at 38 °C.

3.1.2. Effect of Suspension pH on Particle Agglomeration. The pH of an M-PNIPAM 17 kDa suspension was varied from pH 3 to pH 11 using 0.1 M phosphate buffer. Figure 4 shows the transmission values at 40 °C over time, with a reference sample at 25 °C and pH 7. Apparently, a low suspension pH leads to higher agglomeration and sedimentation rates. For pH 3 and pH 5, transmission values reach a maximum after 3 min, whereas the transmission is much lower at pH 11. The same effect is observed for an M-PNIPAM 30 kDa suspension (see the Supporting Information, Figure S8), where agglomeration and consequently transmission were highest at pH 4. This effect can be attributed to a varying surface charge of the particles depending on the pH. A lower surface charge will lead to less electrostatic repulsion and enhanced agglomeration. This was verified with zeta potential measurements, which showed that the point of zero charge of the M-PNIPAM particles was at approximately pH 4. Therefore, it can be concluded that agglomeration increases because there is less electrostatic repulsion at low pH values.

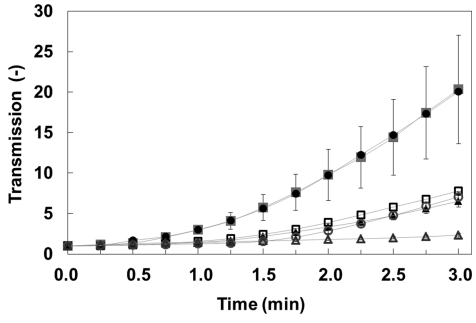

Figure 4. Normalized transmission of M-PNIPAM 17 kDa particle suspension recorded over time at 500 nm. The temperature (40 °C) and particle concentration (4 g/L) was kept constant. The pH of the suspension (0.1 M phosphate buffer) was varied (filled squares, pH 3; filled circles, pH 5; filled triangles, pH 7; empty squares, pH 9; empty circles, pH 11). A sample at 25 °C and pH 7 (empty triangles) is shown for comparison.

3.1.3. Effect of Salts on Particle Agglomeration. The influence of salts (potassium iodide, sodium chloride, and ammonium sulfate) on agglomeration behavior of M-PNIPAM suspensions was investigated. Figure 5 shows transmission values after 3 min of settling at 40 °C. It can be seen that NaCl has virtually no influence on agglomeration, while KI reduces agglomeration and $(NH_4)_2SO_4$ leads to enhanced agglomeration. An increase in salt concentration from 0.5 to 1.0 M leads to a more pronounced effect in the case of $(NH_4)_2SO_4$ and KI. The observed differences can be attributed to the salt type, chaotropic or kosmotropic, and its ability to influence the ordered structure of water molecules around the polymer-coated particles, by either salting in or salting out.[26] Among the salts tested, NaCl is neutral while $(NH_4)_2SO_4$ and KI are kosmotropic and chaotropic, respectively. Therefore, it can be concluded that the interaction of hydrophobic domains in the PNIPAM chains plays an important role in particle agglomeration.

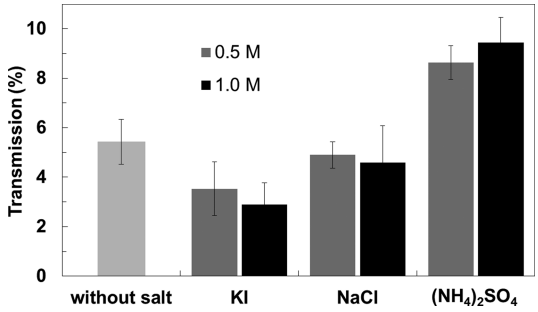

Figure 5. Transmission of M-PNIPAM 17 kDa particle suspension recorded at 500 nm after 3 min of settling. The salt type (KI, NaCl, $(NH_4)_2SO_4$) and concentration (light gray, 0 M; dark gray, 0.5 M; black, 1.0 M) was varied. Testing was done at 40 °C, in 0.1 M phosphate buffer pH 7 and at a particle concentration of 4 g/L.

3.1.4. Recycling of M-PNIPAM Particles. To validate if the thermoresponsive agglomeration of the M-PNIPAM particles is

DOI: 10.1021/acsami.5b02642
ACS Appl. Mater. Interfaces 2015, 7, 14279–14287

reversible, we completed testing as described in Section 2.8. With the aim of simulating a real process for the intended use, the particles were additionally separated after each cycle and fresh buffer was added. Here, possible particle loss should become visible if particles are withdrawn with the supernatant. Figure 6 shows ten heating−cooling cycles of a 4 g/L

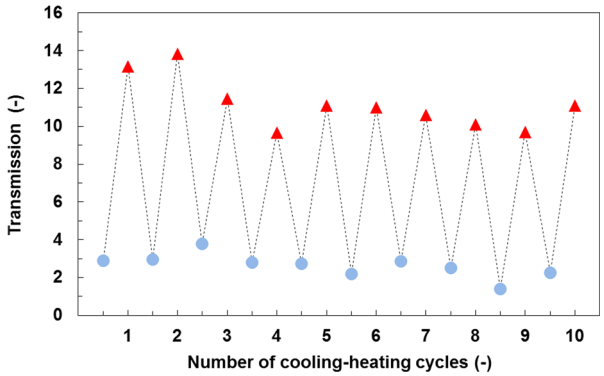

Figure 6. Transmission of M-PNIPAM 17 kDa particle suspension recorded at 500 nm after cooling to 20 °C (blue circles) and after heating to 40 °C (red triangles). After the heating cycle, the particles were magnetically separated and fresh buffer was added. After each of the ten cooling and heating cycles the particles were redispersed. Settle time for all samples prior to measurement was 3 min. The particle concentration was 4 g/L and 0.1 M phosphate buffer at pH 7 was used.

M-PNIPAM 17 kDa suspension. As can be seen, particle agglomeration at 40 °C leads to an increase in transmission values, whereas transmission is low at 20 °C where the suspension is well-dispersed. This occurs consistently for all ten cycles with only slight variations. Therefore, the reversibility of the temperature-switchable agglomeration is confirmed and particles can be recycled without substantial loss.

3.1.5. Magnetic Field-Induced Separation. The thermoresponsive property was introduced to the magnetic particles to enhance separation in external magnetic fields. This was investigated in small scale as described in section 2.9. Figure 7 shows the magnetic separation of unmodified M-PVA (A)

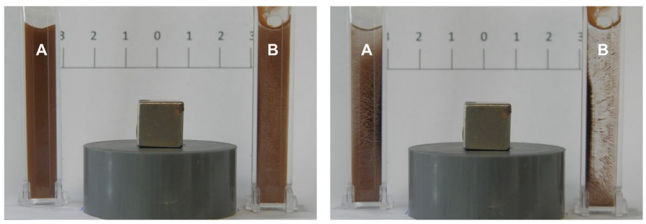

Figure 7. Images of the magnetic separation of particles, recorded 5 s (left) and 30 s (right) after placement next to a small permanent magnet block. Unmodified (A) M-PVA particles and (B) M-PNIPAM 17 kDa particles at 4 g/L in 0.1 M acetate buffer pH 4, at 35 °C.

and M-PNIPAM (B) particles at 35 °C. The pictures were taken 5 s (left) and 30 s (right) after placement next to the magnet. It can be seen that both suspensions are initially well-dispersed. After 30 s, the M-PNIPAM suspension is almost completely separated, whereas the M-PVA suspension is still dispersed. This proves that agglomeration due to thermoresponsive polymer chains has led to enhanced separation of M-PNIPAM particles in the external magnetic field. The magnetic separation at high and low temperature is compared in Figure S9 and Figure S10 (Supporting Information) for M-PVA and M-PNIPAM particles, respectively. Here, a clear influence of the temperature on particle agglomeration is observed for M-PNIPAM particles, while no distinct difference is seen for M-PVA particles. At 35 °C, M-PNIPAM particles are readily separated, whereas at 20 °C separation is very slow because particles disperse well.

Analysis showed that protein binding to M-PNIPAM particles was approximately zero (see Table 1), which means

Table 1. Protein Loading Capacity of Modified Particles Compared with Unmodified M-PVA Particles[a]

particle type	protein loading[b] (mg g^{-1} particle)	desorption[c] (%)
M-PVA	13 ± 0	96 ± 2
M-PNIPAM 17 kDa	0[d]	
M-P(NIPAM-CEA)	57 ± 2	101 ± 9
M-P(NIPAM-SPA)	132 ± 4	97 ± 4

[a]A concentration of 1.5 g/L lactoferrin and a particle concentration of 5 mg/mL were used. The trials were conducted at 20 °C and pH 7. [b]Calculated using eq 4. [c]Relative desorption values were obtained by elution with 1 M NaCl. [d]The calculated loading value was negative due to a measurement uncertainty of the supernatant and initial concentration.

that there was little unspecific adsorption to the PNIPAM-coated particle surface. In the following, the modification of M-PNIPAM particles with ionic monomers is described, which should allow specific protein binding by ion exchange.

3.2. Block Copolymer Particles. A single end-group per PNIPAM chain proved to be insufficient for protein binding (see Supporting Information). The same acrylates used for end-group functionalization were therefore employed in creating a two- and a three-block copolymer of PNIPAM and the respective polyacrylate. The two-block copolymer consists of a thermoresponsive PNIPAM chain (approximately 90%) attached to the particle surface and an ion exchange acrylate chain (approximately 10%) extending outward into the suspension. The three-block copolymer consists of a PNIPAM block (approximately 82%), an acrylate block (approximately 9%), followed by another PNIPAM block (approximately 9%). For block copolymer synthesis, M-PNIPAM 17 kDa particles were subjected to a second and third RAFT polymerization step, respectively, with the particular acrylate or NIPAM, at the conditions described above. Figure 8 shows the reaction scheme of two-block polymer synthesis; Figure 11 shows the three-block synthesis procedure.

3.2.1. Two-Block Copolymer PNIPAM Particles [M-P(NIPAM-CEA) and M-P(NIPAM-SPA)]. The protein loading capacity of M-PVA, M-PNIPAM, M-P(NIPAM-CEA), and M-P(NIPAM-SPA) particles was compared. The protein loading and corresponding desorption results for binding of lactoferrin at 20 °C are given in Table 1. Low adsorption (13 mg protein/g particle) was observed for unmodified M-PVA particles, whereas M-PNIPAM particles showed no protein adsorption. The two-block copolymers, M-P(NIPAM-CEA) and M-P(NIPAM-SPA), showed a high protein loading capacity of 57 mg/g and 132 mg/g, respectively. The desorption yields close to 100% indicate that ionic binding is the dominating source for adsorption. It is assumed that the polymer was present in linear form because the trial was conducted below the LCST of PNIPAM.

DOI: 10.1021/acsami.5b02642
ACS Appl. Mater. Interfaces 2015, 7, 14279−14287

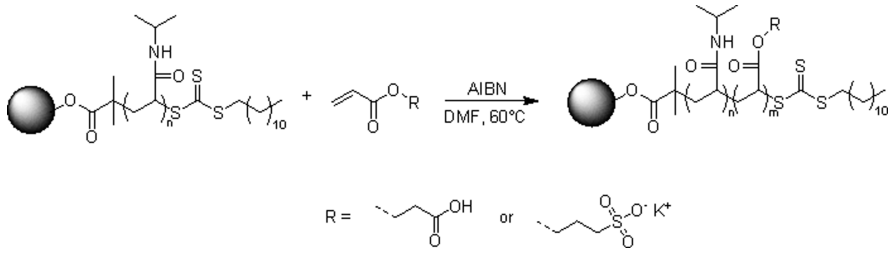

Figure 8. Reaction scheme for "graft-from" RAFT synthesis of two-block copolymer with acrylate monomers CEA and SPA starting from M-PNIPAM 17 kDa particles. "*n*" is the number of NIPAM monomers and "*m*" is the number of acrylate monomers.

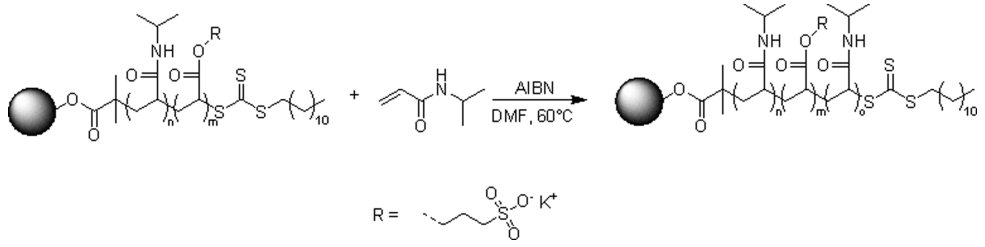

Figure 11. Reaction scheme of "graft-from" RAFT synthesis of three-block copolymer starting from M-P(NIPAM-SPA) particles. "*n*" is the number of NIPAM monomers in the first block, "*m*" is the number of acrylate monomers in the second block, and "*o*" is the number of NIPAM monomers in the third block.

M-P(NIPAM-SPA) particles were chosen for further investigations as these particles showed higher protein adsorption than the M-P(NIPAM-CEA) particles. The temperature dependence of protein adsorption is important for the proposed use as temperature-switchable adsorbents. In Table 2,

Table 2. Protein Loading Capacity of M-P(NIPAM-SPA) Particles Incubated with Protein Solution[a]

protein	temperature (°C)	protein loading[b] (mg g^{-1} particle)	desorption[c] (%)
lactoferrin	20	136 ± 2	94 ± 2
	40	134 ± 2	74 ± 1
lysozyme	20	65 ± 1	101 ± 1
	40	65 ± 1	95 ± 4

[a]A protein concentration of 2 g/L and a particle concentration of 5 mg/mL were used. The trials were conducted at pH 7. [b]Calculated using eq 4. [c]Desorption values were obtained by elution with 1 M NaCl.

the adsorption of lactoferrin and lysozyme to M-P(NIPAM-SPA) particles is compared at 20 and 40 °C. For both proteins, the loading capacity is virtually the same at 20 and 40 °C. The desorption yield is lower at 40 °C than at 20 °C. At a temperature above the LCST, collapsed PNIPAM chains may contribute to protein binding via hydrophobic interaction. These interactions are not weakened by the addition of salt, resulting in incomplete desorption and lower desorption yields.

Adsorption isotherms of lactoferrin are shown in Figure 9, whereas the corresponding Bi-Langmuir fitting parameters are given in Table S1 (Supporting Information). For M-P(NIPAM-SPA), the maximum loading capacity greatly increases and the Langmuir coefficient decreases at both 20 and 40 °C. Thus, the modified particles have a high adsorption capacity and affinity for the protein. The isotherms confirm that protein binding to M-P(NIPAM-SPA) particles is independent of temperature.

Agglomeration was not observed for M-P(NIPAM-SPA) particles up to a temperature of 50 °C (at pH 7 and a particle concentration of 4 g/L). It is well-known that various

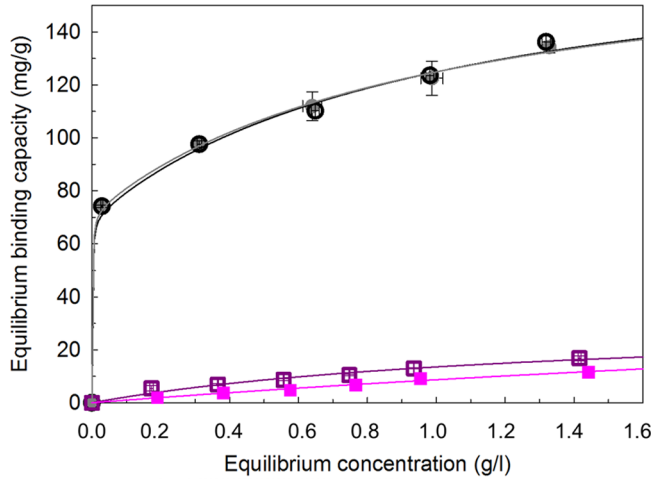

Figure 9. Adsorption of lactoferrin in 0.1 M phosphate buffer pH 7 at 20 °C. Equilibrium binding capacity of unmodified M-PVA particles at 20 °C (empty squares) and 40 °C (filled squares) as well as M-P(NIPAM-SPA) particles at 20 °C (empty circles) and at 40 °C (filled circles), each with the respective Bi-Langmuir isotherm fit. The Bi-Langmuir parameters are given in Table S2 (Supporting Information).

comonomers can alter the LCST of PNIPAM copolymers[27−29] and that the thermoresponsive behavior may disappear completely.[30,31] According to Kuckling et al.,[29] charged copolymers prevent agglomeration of the polymer chains. In the present case, it is assumed that the ionic block (SPA: pK_a 2−2.5[32]) rendered the two-block copolymer particles too hydrophilic to readily agglomerate. However, the particles showed thermoresponsive agglomeration at 40 °C, when lysozyme or BSA was adsorbed to their surface. This is probably due to shielding of the ionic groups by bound protein molecules. Figure 10 shows the transmission curves of M-P(NIPAM-SPA) suspensions at 20 and 40 °C. At 40 °C, the transmission greatly increases over time whereas at 20 °C the transmission stays nearly constant.

DOI: 10.1021/acsami.5b02642
ACS Appl. Mater. Interfaces 2015, 7, 14279−14287

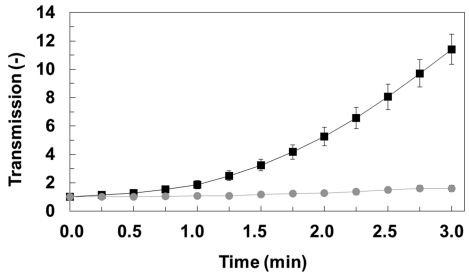

Figure 10. Normalized transmission of M-P(NIPAM-SPA) particle suspensions with adsorbed lysozyme at 20 °C (gray circles) and 40 °C (black squares) recorded over time at 500 nm. Testing was done at pH 7 in 0.1 M phosphate buffer at a particle concentration of 4 g/L.

The thermoresponsive agglomeration behavior of the two-block copolymer particles with adsorbed proteins render them applicable as temperature-switchable adsorbents in the following way: while adsorption takes place in a large volume at a low temperature, followed by enhanced separation due to particle agglomeration at an elevated temperature, elution is conducted in a small volume to concentrate the product. When ammonium sulfate or another kosmotropic salt are used as a desorption agent, agglomeration of particles is enhanced. Particles can then easily be separated by magnetic fields and be reused with fresh feed solution.

3.2.2. Three-Block Copolymer PNIPAM Particles. A third block consisting of PNIPAM was integrated into the polymer chains according to the reaction scheme shown in Figure 11, with the intention of regaining thermoresponsive agglomeration behavior of the unloaded particles. However, even after the introduction of this third block, the unloaded particles did not show temperature induced agglomeration and kept high protein binding capacities (details can be found in the Supporting Information). Both observations are an indication, that the third block of PNIPAM was not able to shield the ionic groups. Another reason for the only slightly reduced protein binding capacity is the fairly high distance between the grafted polymer chains (approximately 6 nm) offering enough space for the proteins to approach the ionic block in the middle of the chain.

4. Conclusions. Thermoresponsive magnetic particles were synthesized via RAFT "graft-from" synthesis. The successful introduction of thermoresponsive polymers was verified by IR spectroscopy and TGA. The M-PNIPAM particles' agglomeration properties were investigated in terms of suspension concentration, pH, temperature and salt addition. Maximum agglomeration of M-PNIPAM suspensions was found at 40 °C in 0.1 M phosphate buffer at pH 3−4 at high particle concentrations. Kosmotropic salt (ammonium sulfate) was found to enhance agglomeration, most likely due to salting out of PNIPAM chains. In all cases, sample agglomeration was measured indirectly by transmission values that increased because of agglomeration and sedimentation of agglomerates. A comparison between modified and unmodified particles served to verify that the observed effects are actually due to the thermoresponsive property. Repeated agglomeration and deagglomeration was demonstrated along with improved separation in an external magnetic field. Protein binding was accomplished by the introduction of ionic copolymers 3-sulfopropyl acrylate and 2-carboxyethyl acrylate. It was shown that binding of lysozyme, BSA, and lactoferrin was independent of temperature. High adsorption capacities were found for both two- and three block copolymer particles, but agglomeration of these particles was only possible when protein was adsorbed. This allows capture of proteins by the well-dispersed copolymer particles at ambient temperature with subsequent selective magnetic separation of particle agglomerates at elevated temperature.

■ ASSOCIATED CONTENT

Supporting Information

Particle characterization data (AGM, ESEM, XRD, magnetic separation) as well as results of end-group functionalization and three-block copolymer synthesis. The Supporting Information is available free of charge on the ACS Publications website at DOI: 10.1021/acsami.5b02642.

■ AUTHOR INFORMATION

Corresponding Author

*E-mail: anja.paulus@kit.edu. Phone: +49 721 608-22984.

Author Contributions

All authors have given approval to the final version of the manuscript.

Notes

The authors declare no competing financial interest.

■ ACKNOWLEDGMENTS

Thank you to Anna-Lena Winkler (KIT-IFG) for carrying out fluorescence microscopy, to Dr. Annett Steudel and Dr. Katja Emmerich (KIT, Competence Center for Material Moisture) for TGA sample analysis, and to Dr. Peter Weidler (KIT-IFG) for XRD measurements. We thank Dr. Markus Delay (KIT-EBI) for help with zeta potential measurements.

■ REFERENCES

(1) Thevenot, J.; Oliveira, H.; Sandre, O.; Lecommandoux, S. Magnetic Responsive Polymer Composite Materials. *Chem. Soc. Rev.* **2013**, *42* (17), 7099−7116.

(2) Schmidt, A. M. Thermoresponsive Magnetic Colloids. *Colloid Polym. Sci.* **2007**, *285* (9), 953−966.

(3) te Riele, P. M.; Verbeek, P. H. J.; Sarkar, A. Method for Separating a Fluid from a Mixture of Fluids using Ferromagnetic Nanoparticles. Patent EP 2731114 A1, 2014.

(4) Borlido, L.; Moura, L.; Azevedo, A. M.; Roque, A. C. A.; Aires-Barros, M. R.; Farinha, J. P. S. Stimuli-Responsive Magnetic Nanoparticles for Monoclonal Antibody Purification. *Biotechnol. J.* **2013**, *8* (6), 709−717.

(5) Medeiros, S. F.; Santos, A. M.; Fessi, H.; Elaissari, A. Stimuli-responsive Magnetic Particles for Biomedical Applications. *Int. J. Pharm.* **2011**, *403* (1−2), 139−161.

(6) Sahoo, B.; Devi, K. S. P.; Banerjee, R.; Maiti, T. K.; Pramanik, P.; Dhara, D. Thermal and pH Responsive Polymer-Tethered Multifunctional Magnetic Nanoparticles for Targeted Delivery of Anticancer Drug. *ACS Appl. Mater. Interfaces* **2013**, *5* (9), 3884−3893.

(7) Lai, J. J.; Hoffman, J. M.; Ebara, M.; Hoffman, A. S.; Estournès, C.; Wattiaux, A.; Stayton, P. S. Dual Magnetic-/temperature-responsive Nanoparticles for Microfluidic Separations and Assays. *Langmuir* **2007**, *23* (13), 7385−7391.

(8) Tsuji, S.; Kawaguchi, H. Thermosensitive Pickering Emulsion Stabilized by Poly(N-isopropylacrylamide)-carrying Particles. *Langmuir* **2008**, *24* (7), 3300−3305.

(9) Kondo, A.; Fukuda, H. Preparation of Thermo-sensitive Magnetic Hydrogel Microspheres and Application to Enzyme Immobilization. *J. Ferment. Bioeng.* **1997**, *84* (4), 337−341.

(10) Aseyev, V.; Tenhu, H.; Winnik, F. M., Non-ionic Thermoresponsive Polymers in Water. In *Self Organized Nanostructures of*

DOI: 10.1021/acsami.5b02642
ACS Appl. Mater. Interfaces 2015, 7, 14279−14287

Amphiphilic Block Copolymers II; Müller, A. H. E., Borisov, O., Eds.; Springer: Berlin, 2011; Chapter 57, pp 29−89.
(11) Lutz, J.-F.; Akdemir, Ö.; Hoth, A. Point by Point Comparison of Two Thermosensitive Polymers Exhibiting a Similar LCST: Is the Age of Poly(NIPAM) Over? *J. Am. Chem. Soc.* **2006**, *128* (40), 13046−13047.
(12) Kanazawa, H.; Okano, T. Temperature-responsive chromatography for the separation of biomolecules. *J. Chromatogr. A* **2011**, *1218* (49), 8738−8747.
(13) Kumar, A.; Srivastava, A.; Galaev, I. Y.; Mattiasson, B. Smart Polymers: Physical Forms and Bioengineering Applications. *Prog. Polym. Sci.* **2007**, *32* (10), 1205−1237.
(14) Moad, G.; Rizzardo, E.; Thang, S. H. Living Radical Polymerization by the RAFT Process. *Aust. J. Chem.* **2005**, *58* (6), 379−410.
(15) Ma, M.; Zheng, S.; Chen, H.; Yao, M.; Zhang, K.; Jia, X.; Mou, J.; Xu, H.; Wu, R.; Shi, J. A Combined ″RAFT″ and ″Graft From″ Polymerization Strategy for Surface Modification of Mesoporous Silica Nanoparticles: Towards Enhanced Tumor Accumulation and Cancer Therapy Efficacy. *J. Mater. Chem. B* **2014**, *2* (35), 5828−5836.
(16) Rahman, M. M.; Elaissari, A. Temperature and Magnetic Dual Responsive Microparticles for DNA Separation. *Sep. Purif. Technol.* **2011**, *81* (3), 286−294.
(17) Panahi, H. A.; Tavanaei, Y.; Moniri, E.; Keshmirizadeh, E. Synthesis and Characterization of Poly[N-isopropylacrylamide-co-1-(N,N-bis-carboxymethyl)amino-3-allylglycerol] Grafted to Magnetic Nano-particles for the Extraction and Determination of Fluvoxamine in Biological and Pharmaceutical Samples. *J. Chromatogr. A* **2014**, *1345* (0), 37−42.
(18) Lai, J. T.; Filla, D.; Shea, R. Functional Polymers from Novel Carboxyl-terminated Trithiocarbonates as Highly Efficient RAFT Agents. *Macromolecules* **2002**, *35* (18), 6754−6756.
(19) Ohno, K.; Ma, Y.; Huang, Y.; Mori, C.; Yahata, Y.; Tsujii, Y.; Maschmeyer, T.; Moraes, J.; Perrier, S. Surface-Initiated Reversible Addition−Fragmentation Chain Transfer (RAFT) Polymerization from Fine Particles Functionalized with Trithiocarbonates. *Macromolecules* **2011**, *44* (22), 8944−8953.
(20) Liu, X. Y.; Zheng, S. W.; Hong, R. Y.; Wang, Y. Q.; Feng, W. G. Preparation of Magnetic Poly(styrene-co-acrylic Acid) Microspheres with Adsorption of Protein. *Colloids Surf., A* **2014**, *443* (0), 425−431.
(21) Munk, T.; Baldursdottir, S.; Hietala, S.; Rades, T.; Nuopponen, M.; Kalliomäki, K.; Tenhu, H.; Rantanen, J.; Strachan, C. J. Investigation of the Phase Separation of PNIPAM using Infrared Spectroscopy together with Multivariate Data Analysis. *Polymer* **2013**, *54* (26), 6947−6953.
(22) Narimani, F.; Zohuriaan-Mehr, M. J.; Kabiri, K.; Bouhendi, H.; Omidian, H.; Najafi, V. Overentrant Swelling Behaviour of Poly-(potassium, 3-Sulfopropyl Acrylate-acrylic Acid) Gels. *J. Polym. Res.* **2012**, *19* (12), 1−8.
(23) Kumar, R. V.; Koltypin, Y.; Cohen, Y. S.; Cohen, Y.; Aurbach, D.; Palchik, O.; Felner, I.; Gedanken, A. Preparation of Amorphous Magnetite Nanoparticles Embedded in Polyvinyl Alcohol using Ultrasound Radiation. *J. Mater. Chem.* **2000**, *10* (5), 1125−1129.
(24) Sousa, R. G.; Magalhães, W. F.; Freitas, R. F. S. Glass Transition and Thermal Stability of Poly(N-isopropylacrylamide) Gels and Some of Their Copolymers with Acrylamide. *Polym. Degrad. Stab.* **1998**, *61* (2), 275−281.
(25) Chen, R. Y.; Yeun, W. Y. D. Review of the High-Temperature Oxidation of Iron and Carbon Steels in Air or Oxygen. *Oxid. Met.* **2003**, *59* (5−6), 433−468.
(26) Zhang, Y.; Cremer, P. S. Interactions Between Macromolecules and Ions: the Hofmeister Series. *Curr. Opin. Chem. Biol.* **2006**, *10* (6), 658−663.
(27) Feil, H.; Bae, Y. H.; Feijen, J.; Kim, S. W. Effect of Comonomer Hydrophilicity and Ionization on the Lower Critical Solution Temperature of N-isopropylacrylamide Copolymers. *Macromolecules* **1993**, *26* (10), 2496−2500.
(28) Klaikherd, A.; Nagamani, C.; Thayumanavan, S. Multi-Stimuli Sensitive Amphiphilic Block Copolymer Assemblies. *J. Am. Chem. Soc.* **2009**, *131* (13), 4830−4838.
(29) Kuckling, D.; Adler, H.-J. P.; Arndt, K.-F.; Ling, L.; Habicher, W. D. Temperature and pH Dependent Solubility of Novel Poly(N-isopropylacrylamide)-copolymers. *Macromol. Chem. Phys.* **2000**, *201* (2), 273−280.
(30) Chen, G.; Hoffman, A. S. A New Temperature- and pH-responsive Copolymer for Possible Use in Protein Conjugation. *Macromol. Chem. Phys.* **1995**, *196* (4), 1251−1259.
(31) Karjalainen, E.; Chenna, N.; Laurinmaki, P.; Butcher, S. J.; Tenhu, H. Diblock Copolymers Consisting of a Polymerized Ionic Liquid and Poly(N-isopropylacrylamide). Effects of PNIPAM Block Length and Counter Ion on Self-assembling and Thermal Properties. *Polym. Chem.* **2013**, *4* (4), 1014−1024.
(32) Janson, J.-C. *Protein Purification: Principles, High Resolution Methods, and Applications*; John Wiley & Sons: New York, 2011; Vol. *151*.

DOI: 10.1021/acsami.5b02642
ACS Appl. Mater. Interfaces 2015, 7, 14279−14287